Light quenching and fluorescence depolarization of Rhodamine B and applications of this phenomenon to biophysics

ARTICLE *in* THE JOURNAL OF PHYSICAL CHEMISTRY · APRIL 1994

DOI: 10.1021/j100052a055

CITATIONS
41

READS
44

4 AUTHORS, INCLUDING:

Joseph R Lakowicz
University of Maryland Medical Center
876 PUBLICATIONS **41,797** CITATIONS
SEE PROFILE

Ignacy Gryczynski
University of North Texas HSC at Fort Worth
366 PUBLICATIONS **9,289** CITATIONS
SEE PROFILE

Józef Kuśba
Gdansk University of Technology
80 PUBLICATIONS **1,179** CITATIONS
SEE PROFILE

Light Quenching and Fluorescence Depolarization of Rhodamine B and Applications of This Phenomenon to Biophysics

Joseph R. Lakowicz,* Ignacy Gryczyński, Valery Bogdanov, and Józef Kuśba

Center for Fluorescence Spectroscopy, Department of Biological Chemistry, School of Medicine, University of Maryland at Baltimore, 108 North Greene Street, Baltimore, Maryland 21201

Received: June 17, 1993; In Final Form: October 11, 1993•

The fluorescence intensity of rhodamine B (RhB) was found to display a sublinear dependence on incident power when excited with the focused output of a cavity-dumped dye laser. This effect was found to be proportional to the amplitude of the emission spectrum at the incident wavelength and to be associated with a decrease in the time-zero anisotropy of RhB. The absence of changes in the intensity decay law or rotational correlation time indicates the absence of photochemical processes. These results are consistent with "light quenching" of RhB due to stimulated emission. In viscous solution the extent of depolarization of the emission was found to be in agreement with theoretical expressions which account for photoselective light quenching and for spatial inhomogeneities in the incident laser beam. The phenomenon of light quenching has numerous potential applications in biophysics, such as studies of the orientation and dynamics of fluorescent macromolecules.

Introduction

Time-resolved fluorescence methods are widely used in chemistry,[1-3] biochemistry, and biophysics.[4,5] In recent years the use of picosecond and femtosecond laser sources and faster detectors has resulted in increased resolution of rapid and/or complex decay processes.[6,7] It is generally assumed that the system under investigation responds linearly to the incident light; that is, the intensity and other spectral parameters are not dependent on the incident power. This assumption is known to be valid for a wide range of experimental conditions.

In the past 2 years there has been increasing interest in the emission induced by simultaneous absorption of two long-wavelength photons, here called two-photon excitation (TPE). While there were earlier reports of TPE, these studies were designed to reveal the symmetry of the electronic states.[8-11] In contrast, the more recent reports used TPE to provide localized excitation in fluorescence microscopy,[12,13] improved resolution of anisotropy decays,[14,15] or resolution of overlapping electronic spectra.[16-18] The surprising observation that TPE can be observed with widely available picosecond laser sources[14-16] is likely to result in the more widespread use of this nonlinear process.

The occurrence of TPE requires locally intense excitation due to the need for simultaneous interaction of the fluorophore with two photons. Under these conditions it is also possible for the fluorophore to undergo stimulated emission. This portion of the emission is not observed with observation at right angles to the incident light. Hence, the observed emission intensity is decreased, and we refer to this phenomena as "light quenching". Until now, light quenching has only been observed when intense Q-switched laser pulses are used, such as the intense pulses from a Ruby laser.[19-21] In the present paper on RhB, and in a recent preliminary report on the laser dye 4-(dicyanomethylene)-2-methyl-6-(*p*-(dimethylamino)styryl)-4*H*-pyran (DCM),[22] we show that significant amounts of light quenching can be observed with high repetition rate picosecond light sources, which are frequently used for studies of time-resolved fluorescence. We do not intend to imply that such data are corrupted by light quenching, which is unlikely with unfocused illumination. Rather, we wish to point out that with focused illumination it is possible to observe light quenching using high repetition rate picosecond dye lasers and that the use of light quenching offers opportunities for novel experiments using time-resolved fluorescence.

The phenomenon of light quenching is shown schematically in Scheme 1. The sample is excited with a pulse of width t_p, the peak power of which can be attenuated with optical filters. In the present experiments, excitation and quenching are due to the same incident beam. Following the incident pulse the resulting emission decays exponentially with a lifetime τ, and at low laser power the total intensity is proportional to the laser power (P). At higher incident power the intensity decay is expected to display the same lifetime τ because the emission occurs after the pulse has passed through the sample ($t_p \ll \tau$). However, the power-normalized intensity (I/P) is expected to be smaller because some fraction of the fluorophores have been stimulated to emit during the pulsed excitation. Hence, one indication of quenching is a sublinear dependence of the emission intensity on incident power.

SCHEME 1: Schematic of the Effects of Intense Pulsed Excitation (Top) on the Intensity (Middle) and Anisotropy Decay (Bottom) of a Fluorophore

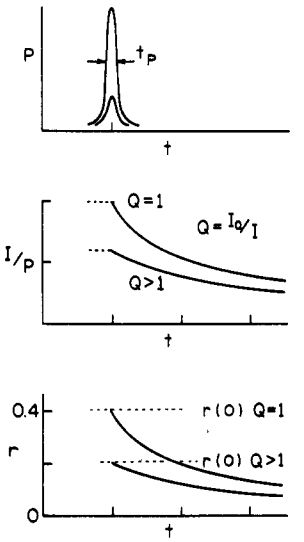

An important aspect of light quenching is that it displays the same photoselection properties as does light absorption. Consequently, light quenching is expected to selectively deplete the population of fluorophores whose transition moments are aligned along the electric vector of the incident light. For vertically polarized excitation (and quenching) and collinear absorption and emission moments, this results in a decrease in the time-zero anisotropy ($r(0)$), as shown in the lower panel of Scheme 1. For a symmetric fluorophore with a single correlation time, the correlation time (Θ) is expected to remain unchanged during

* Author to whom correspondence should be addressed.
• Abstract published in *Advance ACS Abstracts*, December 1, 1993.

0022-3654/94/2098-0334$04.50/0

SCHEME 2: Coordinate System for a Fluorophore

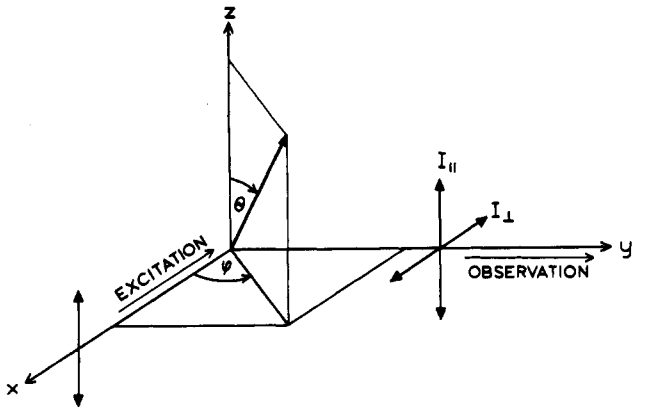

[a] The transition moment makes an angle θ with the Z axis and φ with the X axis.

emission which occurs after passage of the excitation (quenching) pulse, through the observation area.

In the present paper we show that light quenching of RhB can be observed with high repetition rate dye lasers and is accompanied by a decrease in the time-zero anisotropy, with no changes in the decay time or correlation time. We also present a theory for quantitative interpretation of the extent of light quenching and loss of anisotropy which includes consideration of spatial inhomogeneity of the incident laser beam. And finally, we discuss the possible future applications of light quenching in time-resolved fluorescence, biochemistry, and biophysics.

Theory

Light Quenching and Time-Resolved Anisotropy Decays. Suppose the fluorophore's transition dipole makes an angle θ from the vertical axis, and φ from the direction of illumination (Scheme 2). Assume further that the absorption and emission oscillators are collinear and that rotational diffusion does not occur during the lifetime of the excited state. These assumptions are appropriate for long-wavelength excitation of molecules like RhB in a highly viscous solvent. The theory for more complex cases, including rotational diffusion and noncollinear transitions, is now being developed in this laboratory.

The time-dependent anisotropy can be calculated from the excited-state population $n(\theta,t)$ which, assuming that the changes in ground-state population are negligible, is described by

$$\frac{dn(\theta,t)}{dt} = NP\sigma_a \cos^2\theta - n(\theta,t)\left[\frac{1}{\tau} + P\sigma_{lq}\cos^2\theta\right] \quad (1)$$

where N is the ground-state population, σ_a and σ_{lq} are the absorption and light quenching cross sections, respectively, P is the laser power density (photons/(cm^{2}s)), and τ is the unquenched lifetime. In this equation $n(\theta,t)$ represents the number of excited fluorophores, at time t, whose transitions are oriented within the angular interval θ to $\theta + d\theta$. The first term on the right represents the rate of excitation, which depends on $\cos^2\theta$ due to the usual photoselection properties of optical transitions. The second term on the right represents the spontaneous decay rate τ^{-1}, which is independent of angle and the rate of light quenching. This latter quenching rate depends on $\cos^2\theta$. In the case of atomic fluorescence, the absorption and emission are frequently the same, so that $\sigma_a = \sigma_{lq}$. In the case of molecular fluorescence in the fluid phase, there is generally a Stokes' shift, and σ_a and σ_{lq} need not be equal.[25]

Equation 1 is a reflection of an assumption that the excited-state population $n(\theta,t)$ is affected by three competitive processes: excitation, spontaneous decay, and light quenching. The actual value of $n(\theta,t)$ depends on the intensity and length of the incident pulse as well as on the mutual relationship between the rates of excitation ($P\sigma_a\cos^2\theta$), spontaneous decay (τ^{-1}), and light quenching ($P\sigma_{lq}\cos^2\theta$). At very low intensities of excitation the rate of light quenching is small compared to the rate of spontaneous decay ($P\sigma_{lq}\cos^2\theta \ll \tau^{-1}$). The changes in ground-state population are small, and the excited-state population is almost exclusively deactivated by the spontaneous decay. At high excitation intensities (when $P\sigma_a\cos^2\theta \gg \tau^{-1}$) the resulting maximum value of $n(\theta,t)$ strongly depends on the ratio of cross section for light quenching σ_{lq} and the cross section for light absorption σ_a. If σ_{lq} is less or comparable to σ_a, then the total rate of deactivation of the excited state is less or comparable to the rate of excitation. In this case $n(\theta,t)$ becomes relatively large, causing respective large changes in population of the ground state. With N assumed constant eq 1 does not properly describe the kinetics of excitation and deactivation in this case. For high intensities of excitation the applicability of eq 1 is limited to the case when $\sigma_{lq} \gg \sigma_a$. In this case the rate of light quenching may become comparable, larger, or even much larger than the rate of spontaneous decay ($P\sigma_{lq}\cos^2\theta \gg \tau^{-1}$). Light quenching then becomes the main mechanism of deactivation of the excited state. Simultaneously, because $P\sigma_{lq}\cos^2\theta \gg P\sigma_a\cos^2\theta$, the resulting maximum value of $n(\theta,t)$ is much smaller than N, what is tantamount to very small changes in the ground-state population. In this case the excited-state population is small, similarly as for low-intensity excitation, but now, apart from photoselective processes of excitation, the emitted fluorescence is strongly affected by photoselective processes of light quenching. Experimentally, the conditions when $\sigma_{lq} \gg \sigma_a$ may be expected in regions where the absorption is low but near the emission maximum of the fluorophore. Thus, in dyes the most suitable excitation region where the condition $\sigma_{lq} \gg \sigma_a$ may be fulfilled is near the maximum of the emission spectrum, where, due to the Stokes's shift, the absorption spectrum is already very weak.

Suppose the sample is illuminated with a simultaneous excitation and quenching rectangular light pulse of width t_p and with a peak power density P. Then the time-resolved excited fluorophore population at an angle θ is given by

$$n(\theta,t) = \begin{cases} \dfrac{NP\sigma_a\cos^2\theta}{k(\theta)}\{1-\exp[-k(\theta)t]\}, & \text{for } 0 \le t \le t_p \\ \dfrac{NP\sigma_a\cos^2\theta}{k(\theta)}\{1-\exp[-k(\theta)t_p]\}\exp\left(-\dfrac{t-t_p}{\tau}\right), & \text{for } t \ge t_p \end{cases} \quad (2)$$

where

$$k(\theta) = \frac{1}{\tau} + P\sigma_{lq}\cos^2\theta \quad (3)$$

is the total rate of deactivation of the excited state. The first line of eq 1 describes the excited-state population during the light pulse, and the second line describes this population after the light pulse. Note that the term in { } brackets remains constant for $t > t_p$. The time-dependent intensities of the polarized compounds are given by

$$I_\parallel(t) = c\int_0^{2\pi}\int_0^{\pi/2} n(\theta,t)\cos^2\theta\sin\theta\,d\theta\,d\varphi \quad (4)$$

$$I_\perp(t) = c\int_0^{2\pi}\int_0^{\pi/2} n(\theta,t)(1-\cos^2\theta)\cos^2\varphi\sin\theta\,d\theta\,d\varphi \quad (5)$$

where c is a constant. Equations 1–5 allow calculation of the time-resolved anisotropy

$$r(t) = \frac{I_\parallel(t) - I_\perp(t)}{I_\parallel(t) + 2I_\perp(t)} \quad (6)$$

for any value of t.

Light Quenching and Steady-State Anisotropy. The steady-state intensities of the polarized compounds, $I_\parallel$ and $I_\perp$, may be expressed by equations similar to eqs 4 and 5 but with the excited-

SCHEME 3: Relationship between the Pulse Width, Intensity Decay, and Interval between Pulses

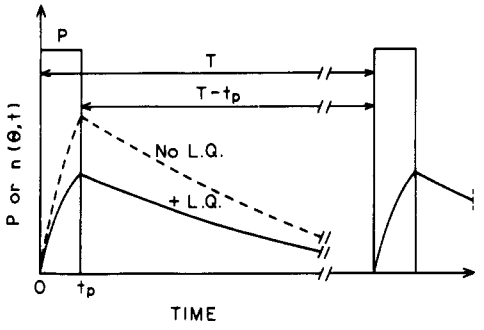

state population $n(\theta,t)$ replaced by its time-averaged value $\bar{n}(\theta)$

$$I_{\parallel} = c\int_0^{2\pi}\int_0^{\pi/2}\bar{n}(\theta)\cos^2\theta\sin\theta\,d\theta\,d\varphi \quad (7)$$

$$I_{\perp} = c\int_0^{2\pi}\int_0^{\pi/2}\bar{n}(\theta)(1-\cos^2\theta)\cos^2\varphi\sin\theta\,d\theta\,d\varphi \quad (8)$$

The time-averaged excited-state population $\bar{n}(\theta)$ may be calculated as

$$\bar{n}(\theta) = \frac{1}{T}\int_0^T n(\theta,t)\,dt \quad (9)$$

where time T is the interval between two consecutive pulses. To avoid any interference of luminescence initiated by different pulses, the population $n(\theta,t)$ should be completely decayed at time $t = T$. That means that time T should satisfy the relation $T - t_p \gg \tau$. The relationship between T and t_p is shown in Scheme 3. The conditions of continuous illumination may be understood on this scheme as corresponding to pulse excitation with t_p, tending to infinity and with fixed length of the interval $T - t_p = \Delta t$, where $\Delta t \gg \tau$. Hence, for continuous illumination, time T is well approximated by time t_p. Expression 9 with $n(\theta,t)$ given by eq 2 yields

$$\bar{n}(\theta) = \frac{\tau NP\sigma_a\cos^2\theta}{Tk(\theta)}\left\{\frac{t_p}{\tau} + \frac{P\sigma_{lq}\cos^2\theta}{k(\theta)}\{1-\exp[-k(\theta)t_p]\}\right\} \quad (10)$$

Equations 7–10 are valid for any value of t_p and allow calculation of the steady-state anisotropy

$$r = \frac{I_{\parallel} - I_{\perp}}{I_{\parallel} + 2I_{\perp}} \quad (11)$$

for any amount of quenching. The above description of the steady-state anisotropy may be simplified in the two limiting cases when excitation and quenching is performed by very short pulses or by the pulses being extremely long, fulfilling in fact the conditions of continuous illumination. These cases will be discussed in the next sections.

The extent of quenching can be described by the parameter $Q = I_0/I$, where $I_0 = I_{\parallel}^0 + 2I_{\perp}^0$ and $I = I_{\parallel} + 2I_{\perp}$ are the fluorescence intensities at the same incident power, in the absence and presence of light quenching, respectively. Computationally, the values of $I_{\parallel}^0$ and $I_{\perp}^0$ can be found from eqs 7 and 8 by setting $\sigma_{lq} = 0$ in eq 10. The value of Q is then calculated using

$$Q = \frac{I_{\parallel}^0 + 2I_{\perp}^0}{I_{\parallel} + 2I_{\perp}} \quad (12)$$

Experimentally, the value of I^0 is determined either by extrapolation to zero incident power or by excitation with an unfocused incident beam.

Steady-State Anisotropy in the Case of Short Pulse Excitation and Quenching. The equations describing the steady-state anisotropy in the case of short pulse excitation and quenching may be obtained from eqs 7–10 as appropriate limits with t_p tending to zero. This type of "steady-state" measurement is performed when a pulse train from a dye laser is used as the excitation source and the steady-state values of $I_{\parallel}$ and $I_{\perp}$ are measured. In order to avoid obtaining a trivial result of the absence of excitation, the limiting procedure has to be carried out with the fixed value of the product Pt_p, which has the meaning of the number of photons passing the unit area of the sample within the single pulse. That means that simultaneously with t_p becoming very small the parameter P has to increase to a very large value. In consequence, in the short pulse limit of eq 10 not only the term t_p/τ but also the terms $1/\tau$ may be omitted [the terms $1/\tau$ are hidden in the rate $k(\theta)$]. Thus, the resulting limiting forms of eqs 7 and 8 are

$$I_{\parallel} = c\frac{2\pi\tau N\sigma_a}{T\sigma_{lq}}\int_0^1[1-\exp(-S_p x^2)]x^2\,dx \quad (13)$$

$$I_{\perp} = c\frac{\pi\tau N\sigma_a}{T\sigma_{lq}}\int_0^1[1-\exp(-S_p x^2)](1-x^2)\,dx \quad (14)$$

where $x = \cos\theta$, $S_p = Pt_p\sigma_{lq}$, and the subscript p is taken to indicate pulsed illumination. These integrals can be evaluated numerically (as done for calculation of Figure 8). After expansion of the exponents into a Maclaurin series and integration over x, one obtains other useful forms of eqs 13 and 14

$$I_{\parallel} = W_p\sum_{k=0}^{\infty}\frac{(-1)^k S_p^{\,k}}{(2k+5)(k+1)!} = \frac{W_p}{5}\left(1 - \frac{5}{14}S_p + \frac{5}{54}S_p^{\,2} - \frac{5}{264}S_p^{\,3} + \ldots\right) \quad (15)$$

$$I_{\perp} = W_p\sum_{k=0}^{\infty}\frac{(-1)^k S_p^{\,k}}{(2k+3)(2k+5)(k+1)!} = \frac{W_p}{15}\left(1 - \frac{3}{14}S_p + \frac{5}{126}S_p^{\,2} - \frac{5}{792}S_p^{\,3} + \ldots\right) \quad (16)$$

where $W_p = 2\pi c\tau NPt_p\sigma_a/T$. On the basis of eqs 15 and 16, one can find the following formula for steady-state anisotropy, valid for short pulse excitation and $S_p \ll 1$

$$r = \frac{2}{5}\left(1 - \frac{9}{70}S_p + \frac{19}{2100}S_p^{\,2} + \frac{36}{67375}S_p^{\,3} + \ldots\right) \quad (17)$$

It is seen from eqs 13 and 14 that if the power density of the incident light tends to infinity (∞) then both polarized intensities, $I_{\parallel}$ and $I_{\perp}$, tend to the same constant value

$$I_{\parallel}^{\infty} = I_{\perp}^{\infty} = c\frac{2\pi\tau N\sigma_a}{3T\sigma_{lq}} \quad (18)$$

Combination of this result with eq 11 implies that for pulse illumination $r \to 0$ when $P \to \infty$.

Steady-State Anisotropy in the Case of Continuous Illumination. If the continuous (c) illumination conditions are assumed, then $t_p \gg \tau$, $T \approx t_p$ (Scheme 3) and eqs 7 and 8 reduce to the form

$$I_{\parallel} = W_c\int_0^1\frac{x^4}{1+S_c x^2}\,dx \quad (19)$$

$$I_{\parallel} = \frac{W_c}{2}\int_0^1\frac{x^2(1-x^2)}{1+S_c x^2}\,dx \quad (20)$$

where $W_c = 2\pi cNP\tau\sigma_a$ and $S_c = P\tau\sigma_{lq}$. We note that continous or quasi-continuous conditions may be obtained when $t_p \approx \tau$, as could occur with a mode-locked ion laser ($t_p \approx 100$ ps) and short-lived fluorophore ($\tau \approx 100$ ps). After integration one obtains

$$I_{\parallel} = \frac{W_c}{3}\left[\frac{1}{S_c} - \frac{3}{S_c^2} + \frac{3}{S_c^{5/2}}\arctan(S_c^{1/2})\right] \quad (21)$$

$$I_{\parallel} = \frac{W_c}{3}\left[\frac{1}{S_c} + \frac{3}{2S_c^2} - \frac{3(S_c-1)}{2S_c^{5/2}}\arctan(S_c^{1/2})\right] \quad (22)$$

Expressions 21 and 22 are identical with those obtained for the same excitation and quenching conditions by Mazurenko.[23] If $S_c \leq 1$, then expansion of the arctan function into a Maclaurin series yields

$$I_{\parallel} = W_c\sum_{k=0}^{\infty}\frac{(-1)^k S_c^k}{2k+5} = \frac{W_c}{5}\left(1 - \frac{5}{7}S_c + \frac{5}{9}S_c^2 - \frac{5}{11}S_c^3 + \ldots\right) \quad (23)$$

$$I_{\perp} = W_c\sum_{k=0}^{\infty}\frac{(-1)^k S_c^k}{(2k+3)(2k+5)} = \frac{W_c}{15}\left(1 - \frac{3}{7}S_c + \frac{5}{21}S_c^2 - \frac{5}{33}S_c^3 + \ldots\right) \quad (24)$$

On the basis of eqs 23 and 24, one can find the following formula for the steady-state anisotropy, valid for continuous excitation and $S_c \ll 1$

$$r = \frac{2}{5}\left(1 - \frac{9}{35}S_c + \frac{23}{175}S_c^2 - \frac{5637}{67375}S_c^3 + \ldots\right) \quad (25)$$

It is easy to see that if $S_c \to \infty$, then expressions 19 and 20 tend to the same limiting value as expressions 13 and 14 [see eq 18]. That means that in the case of continuous illumination $r \to 0$ when $P \to \infty$, similarly as for illumination by pulses.

Steady-State Intensities in Presence of Light Quenching. The extent of light quenching can be characterized by the parameter $Q = I_0/I$, or equivalently by the ratio P/I, where P is the incident power. In general, for any value of the pulse width, the value of the parameter Q can be predicted based on eqs 12 and 7–10. The calculations may be remarkably simplified in the limiting cases of very short ($t_p \ll \tau$) or very long ($t_p \gg \tau$) pulses. For $t_p \ll \tau$ based on eqs 12–16 we obtain

$$I = \frac{W_p}{S_p}\int_0^1[1 - \exp(-S_p x^2)]\,dx = W_p\sum_{k=0}^{\infty}\frac{(-1)^k S_p^k}{(2k+3)(k+1)!} = \frac{W_p}{3}\left(1 - \frac{3}{10}S_p + \frac{1}{14}S_p^2 - \frac{1}{72}S_p^3 + \ldots\right) \quad (26)$$

$$Q_p = S_p\left(3\int_0^1[1 - \exp(-S_p x^2)]\,dx\right)^{-1} = \left(3\sum_{k=1}^{\infty}\frac{(-1)^k S_p^k}{(2k+3)(k+1)!}\right)^{-1} \quad (27)$$

For small amounts of quenching, when $S_p \ll 1$, eq 27 can be rewritten as

$$Q_p = 1 + \frac{3}{10}S_p + \frac{13}{700}S_p^2 - \frac{31}{15750}S_p^3 + \ldots \quad (28)$$

For continuous illumination when $t_p \gg \tau$, one obtains

$$I = W_c\int_0^1\frac{x^2}{1+S_c x^2}\,dx = W_c\left(\frac{1}{S_c} - \frac{1}{S_c^{3/2}}\arctan(S_c^{1/2})\right)$$

$$= W_c\sum_{k=0}^{\infty}\frac{(-1)^k S_c^k}{2k+3} = \frac{W_c}{3}\left(1 - \frac{3}{5}S_c + \frac{3}{7}S_c^2 - \frac{3}{9}S_c^3 + \ldots\right) \quad (29)$$

$$Q_c = \frac{1}{3}\left(\frac{1}{S_c} - \frac{1}{S_c^{3/2}}\arctan(S_c^{1/2})\right)^{-1} = \left(3\sum_{k=0}^{\infty}\frac{(-1)^k S_c^k}{2k+3}\right)^{-1} \quad (30)$$

The series representations in eqs 29 and 30 are valid for $S_c \leq 1$, as well as in eqs 23 and 24. Based on eq 30 it can be shown that for $S_c \ll 1$

$$Q_c = 1 + \frac{3}{5}S_c - \frac{12}{175}S_c^2 + \frac{92}{2625}S_c^3 + \ldots \quad (31)$$

Equations 28 and 31 indicate Stern–Volmer behavior of the light quenching at low intensities of the incident light; that is, I_0/I is linear with incident power at low intensities.

It is clear from the above expressions that for both kinds of illumination, pulsed or continuous, the main parameter describing the effectiveness of light quenching is the number of photons passing the unit area of the sample during the fluorophore lifetime. This is the product Pt_p or $P\tau$, for short pulse or continuous illumination, respectively.

Note that in all series representations of $I_{\parallel}$, $I_{\perp}$, I, r, and Q the first order coefficients for the case of continuous illumination are exactly twice as large as the analogous coefficients for the case of pulse excitation and quenching (Table 1). This behavior can be explained as being a consequence of the fact that at low intensities of the incident light the efficiency of light quenching under the continuous illumination conditions is two times larger than for pulsed illumination. For continuous illumination the excited-state population is practically constant, whereas for weak intensity pulses the excited-state population linearly increases from zero at time $t = 0$ to its maximum value at $t = t_p$, leading to a 2-fold lower time averaged value.

After combination of eq 28 with eq 17 and eq 31 with eq 25 one can obtain the expressions linking the steady-state anisotropies with the amount of quenching Q, which are valid for $(Q-1) \ll 1$. In the case of pulse illumination one obtains

$$r = \frac{2}{5}\left[1 - \frac{3}{7}(Q_p - 1) + \frac{250}{1323}(Q_p - 1)^2 + \ldots\right] \quad (32)$$

and for continuous excitation and quenching

$$r = \frac{2}{5}\left[1 - \frac{3}{7}(Q_c - 1) + \frac{125}{441}(Q_c - 1)^2 + \ldots\right] \quad (33)$$

It is seen from the above equations that for the same extent of quenching ($Q_p = Q_c$), quenching by pulses leads to a lower value of anisotropy. This difference is only apparent at higher amounts of quenching, where the terms second order or higher in Q contribute to the anisotropy.

Spatial Heterogeneity of the Incident Beam. The extent of light quenching depends on the local laser intensity at each point in the observed volume. Hence, for a Gaussian incident beam, one expects more quenching and lower anisotropies at the center of the beam where the power is high, and less quenching and higher anisotropies in the outer region where the incident power is lower. This effect of beam profile on the steady-state anisotropies can be evaluated by assuming that the laser beam is distributed as a Gaussian with distance (ρ) from the center of

TABLE 1: Expressions Describing the Polarized Components, Anisotropy, and the Extent of Light Quenching at Low Intensities of the Incident Beam

	pulse illumination	continuous illumination
$I_\parallel$	$\frac{W_p}{5}\left(1-\frac{5}{14}S_p\right)$	$\frac{W_c}{5}\left(1-\frac{5}{7}S_c\right)$
$I_\perp$	$\frac{W_p}{15}\left(1-\frac{3}{14}S_p\right)$	$\frac{W_c}{15}\left(1-\frac{3}{7}S_c\right)$
I	$\frac{W_p}{3}\left(1-\frac{3}{10}S_p\right)$	$\frac{W_c}{3}\left(1-\frac{3}{5}S_c\right)$
r	$\frac{2}{5}\left(1-\frac{9}{70}S_p\right)$	$\frac{2}{5}\left(1-\frac{9}{35}S_c\right)$
Q	$1+\frac{3}{10}S_p$	$1+\frac{3}{5}S_c$

the beam. Hence, the laser power density becomes

$$P(\rho) = \frac{P_0}{2\pi\delta^2}\exp\left(-\frac{\rho^2}{2\delta^2}\right) \tag{34}$$

where P_0 is the total power in the laser beam and δ is the standard deviation of the spatial power density. With this assumption the polarized steady-state intensities [eqs 13 and 14] observed from a unit area at a distance ρ from the center of the laser beam become

$$i_\parallel(\rho) = c'\frac{2\pi\tau N\sigma_a}{T\sigma_{lq}}\int_0^1\{1-\exp[-S_p(\rho)x^2]\}x^2\,dx \tag{35}$$

$$i_\perp(\rho) = c'\frac{\pi\tau N\sigma_a}{T\sigma_{lq}}\int_0^1\{1-\exp[-S_p(\rho)x^2]\}(1-x^2)\,dx \tag{36}$$

where $S_p(\rho) = P(\rho)t_p\sigma_{lq}$ and c' is a constant. The observed intensities of the parallel and perpendicular components of the emission are given by

$$I_\parallel = \int_0^\infty i_\parallel(\rho)2\pi\rho\,d\rho \tag{37}$$

$$I_\perp = \int_0^\infty i_\perp(\rho)2\pi\rho\,d\rho \tag{38}$$

These integrals can be evaluated numerically. An example of this type of calculation is shown by the dashed line in Figure 7 for the Gaussian (G) light distribution.

Cross Section for Light Quenching. The cross section for quenching (σ_{lq}) is determined by the intrinsic rate of emission Γ, which is the inverse of the natural lifetime ($\tau_N = 1/\Gamma$), and by the overlap of the emission spectrum with the incident wavelength ($\lambda_{ex} = \bar{\nu}_{ex}^{-1}$),[24,25]

$$\sigma_{lq} = \frac{K}{\tau_N}\frac{I(\bar{\nu}_{ex})}{\int I(\bar{\nu})\,d\bar{\nu}} \tag{39}$$

where K is a constant and $\bar{\nu}$ is the wavenumber in cm^{-1}.

Materials and Methods

The light source was the cavity-dumped output of a rhodamine 6G (R6G) dye laser, which was pumped by the 514-nm output of a mode-locked Argon ion laser. The excitation was polarized vertically, as occurs from the output of our argon ion and dye lasers. The observation path length was about 2 nm, as determined by a spatial filter. The pulse width of the dye laser was near 5 ps and was focused to a spot size of about 20 μm in diameter. Hence, an incident power of 50 mW corresponds to a maximum intensity of 1.0×10^9 W/cm^2. The observation was done in the L-format, i.e., 90° through a 0.2-mm slit, located in the center of the waist at the focused laser beam. The 20-fold magnified image of the observed fluorescence spot was a rectangular 4 mm long and 0.4 mm wide and did not display obvious spatial heterogeneity; that is, the illumination appeared to be uniform. Without focusing the spot size was about 0.2 cm in diameter.

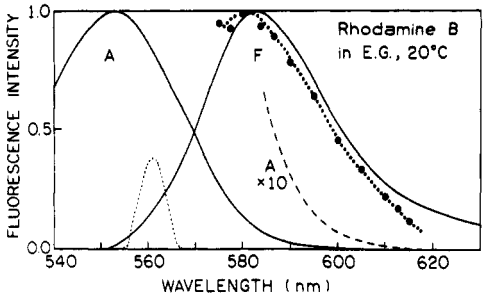

Figure 1. Absorption (A) and emission (F) spectra of rhodamine B in ethylene glycol at 20 °C. The symbols (●) on the emission spectrum show the relative light quenching cross sections $(Q-1)/P$. The emission of RhB was isolated using a 560-nm interference filter (--).

In order to determine if sample heating altered the data, the total power was decreased without changing the instantaneous power. This was accomplished by the use of a low-speed mechanical light chopper in the excitation beam, by which the average intensity was decreased 10–50-fold. The peak power of the incident light was varied by insertion of neutral density filters into the excitation beam. The samples, except glycerol, were stirred during the measurements. We observed no effects of illumination time on the intensity or anisotropy values. The signals were stable upon continuous illumination at our experimental conditions.

All intensity, anisotropy, and frequency-domain (FD) data were obtained using the instrumentation described previously.[26-28] The detector was a red-sensitive R928 PMT from Hamamatsu. The emission was observed through a 560-nm interference filter, 10-nm band pass. For intensity and intensity decay measurements the emission polarizer was 54.7° from the vertical. Control measurements using solvents without RhB gave signals less than 0.5% of the RhB emission, for all polarization conditions and excitation (quenching) wavelengths. RhB was obtained from Exciton, laser grade, and used without further purification. Concentration of RhB in solutions was about 10^{-5} M. Intensity decays were analyzed by least squares[29] in terms of the single decay time model

$$I(t) = I(0)e^{-t/\tau} \tag{40}$$

where $I(0)$ is the intensity at $t = 0$ and τ is the decay time. Anisotropy decays were analyzed[30] in terms of a single correlation time

$$r(t) = r(0)e^{-t/\Theta} \tag{41}$$

where $r(0)$ is the time-zero anisotropy and Θ is the rotational correlation time.

Results

Stationary Measurements of Light Quenching. Absorption and emission spectrum of RhB are shown in Figure 1. The fluorophore is convenient for studies of light quenching because the long-wavelength absorption tail allows excitation from 575 to 615 nm. These wavelengths are available from our R6G dye laser and overlap the emission spectrum of RhB. Such overlap is needed for light quenching (eq 15).

The fluorescence intensities of RhB are shown in Figure 2. For focused excitation the emission intensity does not increase linearly with incident power (lower panel). The relative cross section for quenching (σ_{lq}) can be calculated from a plot of P/I versus laser power (P), where I is the fluorescence intensity. At

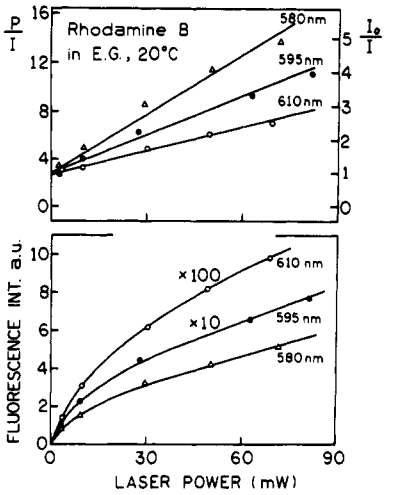

Figure 2. Dependence of the rhodamine B fluorescence intensity on the laser power for selected wavelengths of the excitation (quenching) light (lower panel). The upper panel shows the corresponding Stern–Volmer plots. In all experiments the steady-state intensities or intensity decay data were obtained using magic-angle polarization conditions.

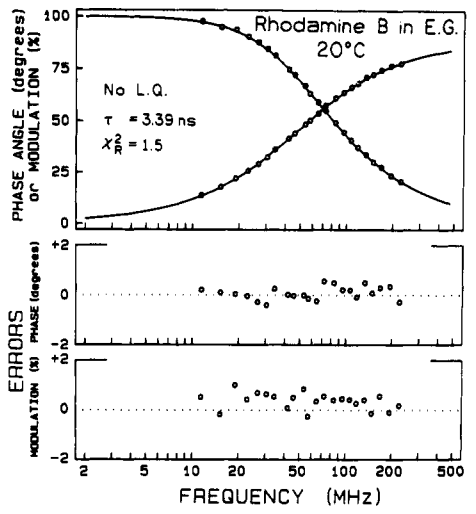

Figure 3. Frequency-domain intensity decay data for rhodamine B in ethylene glycol at 20 °C. The light quenching was eliminated (significantly reduced) by a 20-fold attenuation of peak laser power using a neutral density filter.

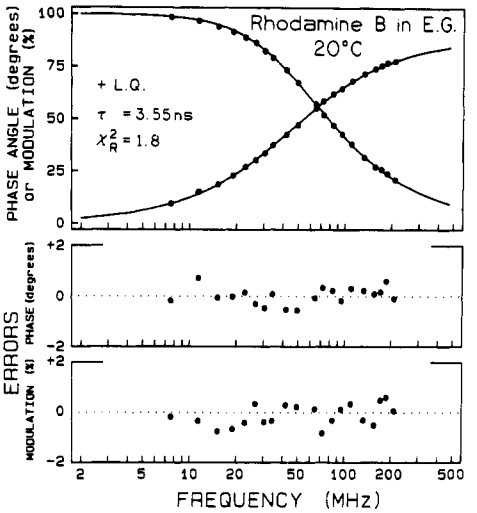

Figure 4. Frequency-domain intensity data for rhodamine B in ethylene glycol at 20 °C, in the presence of light quenching ($Q = 3.2$). In Figure 3 and this figure, the solid lines show the best single exponential fits, and the lower panels, the phase and modulation deviations.

low laser power there is no light quenching, so $I = I_0$, the unquenched emission intensity. In this way the extent of light quenching ($Q = I_0/I$) can be presented as a "Stern–Volmer" plot. For small amounts of quenching (eq 28) the relative cross section for quenching (σ_{lq}) is proportional to the slope of the Stern–Volmer plot (Figure 2, upper panel). The relative values of σ_{lq} are seen to decrease as the incident wavelength increases.

The wavelength-dependent RhB cross sections for light quenching are shown in Figure 1 (●). These relative values are seen to be proportional to the amplitude of the emission spectrum at the quenching wavelength, as expected from eq 39. The fact that the cross sections follow the emission spectrum strongly suggests that we are observing light quenching rather than some other photochemical effect. We were unable to measure the light quenching contents at shorter wavelengths for two reasons. The first is the limited wavelength range of the R6G dye laser used for illumination. Second, even if shorter wavelengths were available, it would be difficult to interpret the results because of increases in the cross section for absorption, decreases in the cross section for quenching, and the possibility of ground-state depletion.

Time-Resolved Studies of Light Quenching. Because of the high illumination intensities needed for light quenching, control experiments are necessary to eliminate the possibility of undesired photochemical or thermal effects. In all the above experiments, the emission spectra were unchanged for high- and low-power illumination, and when the average (not peak) power was decreased 10–50-fold using a slow speed light chopper. For dye laser pulse repetition rates below 4 MHz, the power per pulse is relatively constant. Hence, the average power incident on the sample can also be decreased by decreasing the cavity-dumped rate below 4 MHz. In our opinion, the most definitive control experiments are measurement of lifetimes, correlation times, and $t = 0$ anisotropies ($r(0)$), in the absence and presence of light quenching. For the single-wavelength experiments described above, we expect the lifetimes and correlation times to remain unchanged but expect the $t = 0$ anisotropies to decrease due to selective quenching of the vertically polarized excited-state population.

The frequency-domain intensity decays of RhB are shown in Figure 3 and 4, in the absence and presence of light quenching, respectively. The RhB intensity decay remains a single exponential in the presence of light quenching (Table 2). In the presence of light quenching there is a small increase in mean lifetime, from 3.39 to 3.55 ns, which is presently not understood. These intensity decay data for RhB suggest there are no significant photochemical effects. While the incident power levels are high, there is only weak absorption by the samples, and the absorbed power is apparently not excessive. We note that even if there is a transient rise in temperature around the fluorophore, this effect appears to dissipate within the 3.5-ns lifetime of the excited state and does not significantly alter the lifetime or correlation time for the unquenched values.

TABLE 2: Fluorescence Intensity and Anisotropy Decay Parameters of Rhodamine B in the Absence and Presence of Light Quenching

		intensity decay		anisotropy decay		
solvent; condition[a]	Q	τ (ns)	χ_R^2	r_0	Θ (ns)	χ_R^2
ethylene glycol; 20 °C, no LQ	1.0	3.39	1.5	0.381	3.60	1.7
+ LQ	3.2	3.55	1.8	0.248	3.66	1.3
glycerol; 5 °C, no LQ	1.0	3.61	2.4			
+ LQ	3.2	3.66	2.1			

[a] LQ = light quenching.

The theory for light quenching predicts a decrease in the time-zero anisotropy, with no change in the correlation time. In order to test this prediction, we measured the frequency-domain (FD) anisotropy decay of RhB, in the absence (○) and presence (●) of light quenching (Figure 5). The experimental conditions were

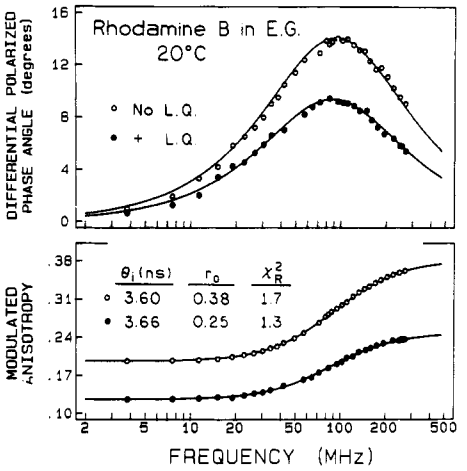

Figure 5. Frequency-domain anisotropy decay data for rhodamine B in ethylene glycol at 20 °C. In the presence of light quenching (Q = 3.2) (●), the time-zero anisotropy is reduced from 0.38 to 0.25. The correlation time is unchanged.

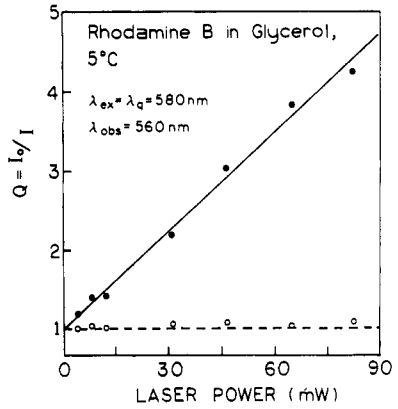

Figure 6. Stern–Volmer representation of the light quenching data for rhodamine B in glycerol at 5 °C (●). The dashed line (–O–) shows the RhB intensities obtained with unfocused laser excitation.

chosen from the results in Figure 2, which showed significant amounts of light quenching for 70-mW excitation at 580 nm. The FD anisotropy data show a uniform decrease in the differential phase angles and modulated anisotropies, which is expected for an apparent decrease in the fundamental anisotropy. Least-squares analysis of these data indicates no change in the rotational correlation time, but a 34% decrease in the time-zero anisotropy from 0.38 to 0.25. Sample heating or other photothermal or photochemical effects are likely to result in more complex changes in the intensity or anisotropy decays. These data (Figure 3–5) are consistent with our model of single beam (pulse) light quenching.

Steady-State Anisotropies and Comparison with Theory. We compared the extent of depolarization caused by light quenching with that predicted by our theory (eqs 11–14). For this comparison we used the anisotropies of RhB in glycerol at 5 °C. In this solvent there is little rotational diffusion during the 3.6-ns lifetime of RhB, allowing direct comparison with our theory which does not consider rotational diffusion. Significant amounts of light quenching of RhB were observed in glycerol (Figure 6), and the relative cross sections for quenching are proportional to the emission spectra (data not shown). Importantly, no light quenching was observed if the laser beam was not focused (Figure 6, –O–).

The steady-state anisotropies of RhB are shown in Figure 7, in glycerol (top) and in ethylene glycol (bottom). The anisotropy (●) decreased progressively with the incident power in both solvents. No change in anisotropy was observed if the laser beam was not focused (O). The extent of depolarization was initially

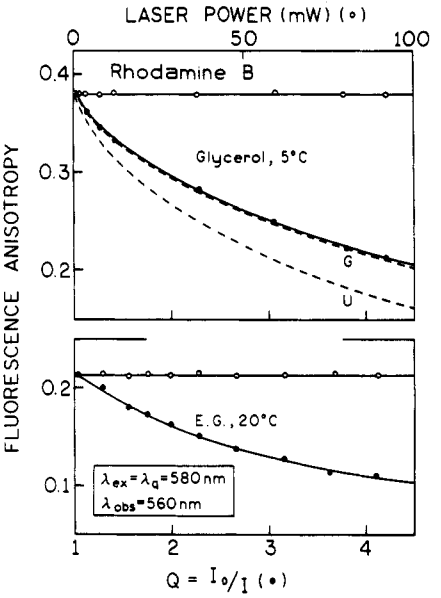

Figure 7. Steady-state anisotropies of RhB in glycerol (top) and ethylene glycol (bottom) observed with focused illumination. The open dots (–O–) show the anisotropies measured with unfocused laser illumination where there is no light quenching (I_0/I = 1.0). The dashed line shows the theoretical prediction for a uniform (U) or a Gaussian (G) beam profiles.

found to be less than that predicted from eqs 11–14 for a uniform (u) distribution (--). However, we realized that it was necessary to account for the spatial distribution of the incident light in the sample. We assumed that the laser beam intensity was distributed as a Gaussian. With this assumption, the observed anisotropies were in precise agreement with that predicted by eqs 34–38. We note that if $t_P \ll \tau$, the calculation is not sensitive to the precise values of t_p, τ, or σ_{lq}, but rather the anisotropy is determined mostly by the amount of quenching. While we are rather certain that it will be necessary to consider the spatial distribution of the incident light, for quantitative interpretation of the results of light quenching experiments. However, we feel the precise agreement shown in Figure 7 is fortuitous given the approximations made in estimating the spatial distribution and intensity of the incident light.

Light Quenching by Pulses and Stationary Illumination. An interesting aspect of light quenching is that the loss in anisotropy depends not only on the amount of quenching Q, but also on whether that quenching was due to pulsed or continuous illumination. This difference is illustrated in Figure 8, showing that illumination with a train of pulses (—) results in a larger decrease in anisotropy than does continuous illumination (--). The curves on Figure 8 were obtained from eq 1, with $I_\parallel$ and $I_\perp$ given by eqs 13 and 14 or by eqs 19 and 20 for pulse or continuous illumination, respectively. For low values of Q the curves can be also obtained from simpler eqs 32 and 33. The fact that quenching by pulses is more effective in depolarization can be understood by considering the effect of a time-delayed quenching pulse (as is illustrated below in Figure 11 and the Discussion). In this case some of the emission occurs prior to arrival of the quenching pulse, and the anisotropy of this emission is unchanged. Quenching by continuous illumination allows some of the emission to occur prior to quenching and hence without a decrease in the anisotropy of this fraction of the emission.

Discussion

The experiments described above demonstrated that light quenching can be significant with use of practical laser sources and without photochemical damage. This observation caused us to speculate how this phenomenon could be used to obtain information about the dynamics of fluorophores in solution and

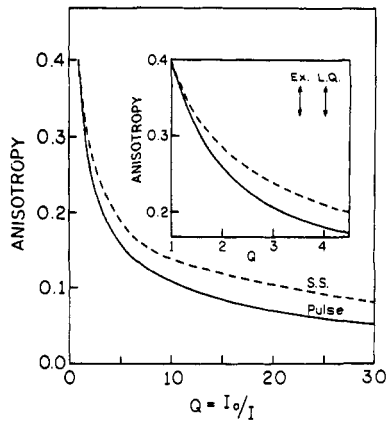

Figure 8. Dependence of fluorescence anisotropy on the amount of quenching $Q = I_0/I$ for one beam experiment (—), assuming no rotational diffusion during the lifetime of the excited state. For the calculations (—) we assumed a pulse width of $t_p = 5$ ps and a decay time of $\tau = 3.5$ ns, to be comparable with the experimental results. The dashed line (--) shows the anisotropy predicted for stationary quenching by continuous illumination, as described by Mazurenko.[23]

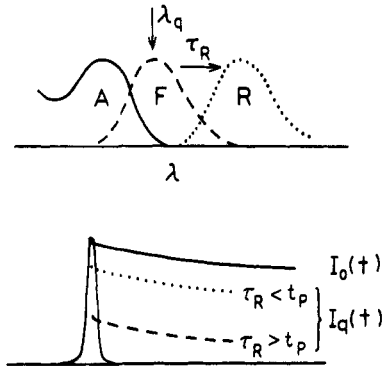

Figure 9. Light quenching and time-dependent spectral relaxation.

in biological macromolecules. The experiments described in this report used the same light pulses for excitation and quenching. Consequently, the light quenching process depends on the spectral properties of the fluorophores as they exist during passage of the light pulse. For instance, suppose RhB was replaced with a more solvent sensitive fluorophore which displayed a Stokes' shift such that the emission spectrum was shifted beyond the excitation and quenching wavelength (longer than 575–615 nm in Figure 1). Then, the extent of quenching would depend on the instantaneous fluorescence intensity at the incident wavelength during the duration of the incident pulse. This concept is illustrated in Figure 9, where F represents the initially excited state (Frank–Condon state), R the solvent relaxed state, and τ_R the spectral or solvent relaxation time. Larger amounts of light quenching are expected in nonpolar solvents or in viscous solvents where $\tau_R > t_p$ (Figure 9, lower panel), where the emission spectrum overlaps with the incident wavelength (Figure 9, upper panel). The amount of quenching is expected to be less if the relaxation is rapid, $\tau_R < t_p$, so that the emission spectrum is already shifted to longer wavelengths during the duration of the incident pulse. It is important to note that, in principle, such experiments contain information on processes which occur on the time scale of the pulse width t_p. Hence, with the availability of picosecond and femtosecond lasers, one can use the amounts of light quenching observed, *under stationary conditions*, to study processes which occur on the picosecond or femtosecond time scale. Such experiments do not require that the fluorophore display a long-wavelength absorption tail, as occurs for RhB. We have recently studied the probe tetraphenylbutadiene (TPB) which displays a substantial Stokes' shift.[31] In this case TPB was excited at wavelengths overlapping its emission by the use of two-photon excitation.

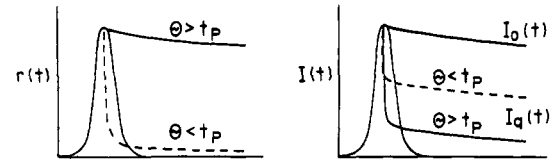

Figure 10. Light quenching and rotational diffusion.

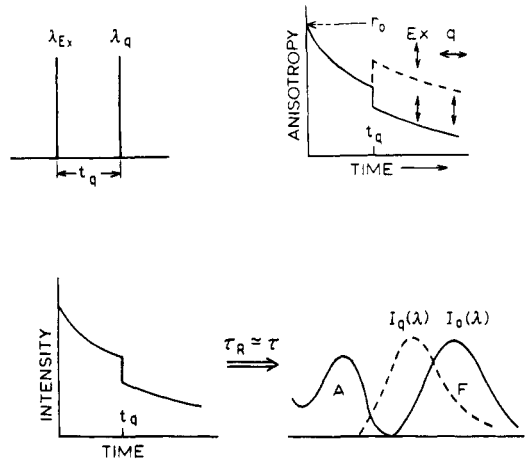

Figure 11. Light quenching with a time-delayed quenching pulse.

Similar reasoning indicates that the single beam light quenching experiments can reveal the rates of fluorophore motion, or more rapid rotations of the electronic moments,[32-34] from the extent of light quenching. This possibility is illustrated in Figure 10, where we assumed the incident light was vertically polarized and the absorption and emission transitions are parallel. Suppose the rotational correlation time (Θ) is long relative to t_p, $\Theta > t_p$ (Figure 10, left, —). Then the excited fluorophores remain favorably oriented to be quenched by the incident beam during the duration of the pulse (lower line, —, right). In contrast, assume the molecules rotate significantly during the time t_p. In this case the excited fluorophore can rotate during the pulse (--, left) resulting in less light quenching (Figure 10, right --). The "rotation" process can be actual rotation diffusion of the fluorophore, which can be studied with subnanosecond and picosecond lasers, or more rapid electronic processes,[32-34] which can be studied with femtosecond lasers. As in the case of spectral relaxation, the time resolution of these light quenching experiments is determined by the pulse width and not the detector or associated electronic circuits.

In our opinion, some of the most remarkable opportunities for light quenching result from the use of separate excitation (Ex) and quenching (q) pulses, as are illustrated schematically in Figure 11. A quenching pulse at time t_q can result in an instantaneous decrease in the fluorescence intensity (lower left), which in effect reduces the mean decay time of the sample. If the spectral relaxation time is comparable to the mean lifetime, then one expects the emission spectrum to display a blue shift upon light quenching (lower right). The anisotropy can also be altered by the quenching pulse. If the absorption and emission moments are parallel, a vertically polarized quenching pulse creates an instantaneous decrease in anisotropy, and a horizontally polarized quenching pulse increases the anisotropy (--, upper right).

The illustration of light quenching in Figure 11 suggests the use of time-resolved measurements to measure the perturbed decays of intensity of anisotropy. While such measurements may be informative, considerable information is available from stationary measurements of the emission spectrum or anisotropy in the presence and absence of the quenching pulse. Recall that the steady-state anisotropy and emission center of gravity ($\bar{\nu}_{cg}$) are averages of the time-resolved values over the lifetime of the

samples,

$$r = \frac{\int_0^\infty r(t)\, I(t)\, dt}{\int I(t)\, dt} \quad (42)$$

$$\bar{\nu}_{cg} = \frac{\int_0^\infty \bar{\nu}_{cg}(t)\, I(t)\, dt}{\int_0 I(t)\, dt} \quad (43)$$

where $\bar{\nu}_{cg}(t)$ is the time-resolved emission center-of-gravity on the wavenumber scale. Light quenching by a delayed quenching pulse can be used to vary the intensity decay $I(t)$ and thereby alter the time available for rotational diffusion or spectral relaxation, providing "lifetime-resolved" measurements of the steady-state anisotropy and the emission spectrum.

Lifetime-resolved measurements offer significant experimental advantages. In previous studies we have used collisional quenching of fluorescence to decrease the decay times of fluorophores bound to proteins or membranes. Steady-state measurements under quenching conditions have been used to measure segmental motions of tryptophan residues in proteins,[35,36] hindered motions of diphenylhexatriene and perylene in lipid bilayers,[37,38] and spectral relaxation of solvent-sensitive probes bound to membranes.[39] We note that in contrast to collisional quenching, light quenching is rapidly reversible by blocking of the quenching beam. Hence, it will be possible to use lock-in amplifiers, homodyne and heterodyne phase sensitive detectors,[40] and other electronic filtering methods to detect small changes in the emission in response to periodic perturbation by the quenching beam.

In summary, light quenching of fluorescence provides a new method for study of the picosecond and femtosecond dynamics of fluorophores and macromolecules, as revealed by their fluorescence emissions. The use of light to control the intensity and anisotropy decay of fluorophores can be regarded as part of the increasing use of light to control a chemical or physical process. For example, light quenching could be used to induce nonzero anisotropies in systems where the anisotropy is initially zero, allowing subsequent time-resolved measurements of the anisotropy decay. Other examples include the use of light to control chemical reactions[41-43] and the use of intense light beams to act as "optical tweezers" which provide controlled trapping or movement of bacteria or subcellular organelles.[44,45] Light quenching is less developed than these topics, but one cannot predict the long-range application of controlling decay times by long-wavelength illumination.

Acknowledgment. This work was performed with support from the National Science Foundation (Grant BIR-9319032) with support for instrumentation from the National Institutes of Health (Grants RR-08119 and RR-07510).

References and Notes

(1) Winnik, M. A., Ed. *Photophysical and Photochemical Tools in Polymer Science*; D. Reidel Publishing Co.: Dordrecht, Holland, 1986.
(2) Warner, I. M., McGown, L. B., Eds. *Advances in Multidimensional Luminescence*; JAI Press, Inc.: Greenwich, CT, 1991; Vol. 1.
(3) Fleming, G. R. *Chemical Applications of Ultrafast Spectroscopy*; Oxford University Press: New York, 1986.
(4) Dewey, T. G. *Biophysical and Biochemical Aspects of Fluorescence Spectroscopy*; Plenum Press: New York, 1991.
(5) Lakowicz, J. R., Ed. Time-Resoled Laser Spectroscopy in Biochemistry III. *Proceedings of SPIE*; SPIE: Bellingham, WA, 1992; Vol. 1640.
(6) Birch, D. J. S.; Imhof, R. E. In *Topics in Fluorescence Spectroscopy Volume 1: Techniques*; Lakowicz, J. R., Ed.; Plenum Press: New York, 1991; Chapter 1.
(7) Small, E. W. In *Topics in Fluorescence Spectroscopy Volume 1: Techniques*; Lakowicz, J. R., Ed.; Plenum Press: New York, 1991; Chapter 2.
(8) McClain, W. M. *J. Chem. Phys.* **1971**, *55*, 2789.
(9) Aleksandrov, A. P.; Bredikhin, V. I.; Genkin, V. N. *Sov. Phys.—JETP* **1971**, *33*, 1078.
(10) McClain, W. M. *J. Chem. Phys.* **1971**, *55*, 2789.
(11) Wirth, M. J.; Koskelo, A.; Sanders, M. J. *Appl. Spectrosc.* **1981**, *35*, 14.
(12) Denk, W.; Strickler, J. H.; Webb, W. W. *Science* **1990**, *248*, 73.
(13) Piston, D. W.; Sandison, D. R.; Webb, W. W. Time-resolved fluorescence imaging and background rejection by two-photon excitation in laser scanning microscopy. *SPIE* **1992**, *1640*, 379–389.
(14) Lakowicz, J. R.; Gryczynski, I.; Danielsen, E. *Chem. Phys. Lett.* **1992**, *191*, 47.
(15) Lakowicz, J. R.; Gryczynski, I.; Gryczynski, Z.; Danielsen, E.; Wirth, M. J. *J. Phys. Chem.* **1992**, *96*, 3000.
(16) Lakowicz, J. R.; Gryczynski, I.; Danielsen, E.; Frisoli, J. K. *Chem. Phys. Lett.* **1992**, *194*, 282.
(17) Rehms, A. A.; Callis, P. R. *Chem. Phys. Lett.*, in press.
(18) Callis, P. R. *J. Phys. Chem.*, in press.
(19) Galanin, M. D.; Kirsanov, B. P.; Chizhikova, Z. A. *Sov. Phys.—JETP Lett.* **1969**, *9*, 502.
(20) Peretti, P.; Ranson, P. *Opt. Commun.* **1971**, *3*, 62.
(21) Butko, A. I.; Voropai, E. S.; Zholnerevich, I. I.; Saechnikov, V. A.; Sarzhevskii, A. M. *Izv. Akad. Nauk SSSR, Ser. Fiz.* **1978**, *42*, 626; (Engl. *Transl.*) 150.
(22) Gryczynski, I.; Bogdanov, V.; Lakowicz, J. R. *Biophys. Chem.*, in press.
(23) Mazurenko, Y. T. *Opt. Spectrosc.* **1973**, *35*, 137.
(24) Butko, A. I.; Voropai, E. S.; Gaisenok, V. A.; Saechnikov, V. A.; Sarzhevskii, A. M. *Opt. Spectrosc.* **1982**, *52*, 153.
(25) Svelto, O. *Principles of Lasers*; Plenum Press: New York, 1989; pp 52, 331.
(26) Lakowicz, J. R.; Maliwal, B. P. *Biophys. Chem.* **1985**, *21*, 61.
(27) Lakowicz, J. R.; Laczko, G.; Gryczynski, I. *Rev. Sci. Instrum.* **1986**, *57*, 2499.
(28) Laczko, G.; Lakowicz, J. R.; Gryczynski, I.; Gryczynski, Z.; Malak, H. *Rev. Sci. Instrum.* **1990**, *61*, 2331.
(29) Lakowicz, J. R.; Gratton, E.; Laczko, G.; Cherek, H.; Limkeman, M. *Biophys. J.* **1984**, *46*, 463.
(30) Maliwal, B. P.; Hermitter, A.; Lakowicz, J. R. *Biochim. Biophys. Acta* **1986**, *873*, 173.
(31) Gryczynski, I.; Bogdanov, V.; Lakowicz, J. R. *J. Fluoresc.*, in press.
(32) Meyers, A. B.; Pereira, M. A.; Holt, P. L.; Hochstrasser, R. M. *J. Chem. Phys.* **1987**, *86*, 5146.
(33) Hansen, J. E.; Rosenthal, S. J.; Fleming, G. R. *J. Chem. Phys.* **1992**, *96*, 3034.
(34) Lakowicz, J. R.; Bogdanov, V.; Kuśba, J.; Gryczynski, I. Manuscript in preparation.
(35) Lakowicz, J. R.; Maliwal, B.; Cherek, H.; Balter, A. *Biochemistry* **1983**, *22*, 1741.
(36) Lakowicz, J. R.; Maliwal, B. *J. Biol. Chem.* **1983**, *258*, 4794.
(37) Lakowicz, J. R.; Knutson, J. R. *Biochemistry* **1980**, *19*, 905.
(38) Lakowicz, J. R.; Prendergast, F. G.; Hogen, D. *Biochemistry* **1979**, *18*, 520.
(39) Lakowicz, J. R.; Hogen, D. *Biochemistry* **1981**, *20*, 1366.
(40) Lakowicz, J. R.; Cherek, H. *J. Biochem. Biophys. Methods* **1981**, *5*, 19.
(41) Potter, E. D.; Herek, J. L.; Pedersen, S.; Liu, Q.; Zewail, A. H. *Nature* **1992**, *355*, 66.
(42) Maddox, J. *Nature* **1992**, *360*, 103.
(43) Smith, I. W. M. *Nature* **1992**, *358*, 279.
(44) Block, S. M.; Blair, D. F.; Berg, H. C. *Cytometry* **1991**, *12*, 492.
(45) Ashkin, A.; Dziedzic, J. M.; Yamane, T. *Nature* **1987**, *330*, 769.